UNIVERSITY OF Southampton

Engineering and the Environment

Aeronautics, Astronautics and Computational Engineering

Multi-fidelity strategies for combustor design using co-Kriging of spatio-temporal combustion dynamics

UTC for Computational Engineering

Moresh Wankhede, Neil Bressloff and Andy Keane, Faculty of Engineering and the Environment

Marco Zedda, Rolls-Royce plc.

Introduction

The objective of meeting stricter NOx emission requirements has been leading the development of aero-engine combustors over many years. Moreover, this need to reach very low emission limits is changing several aspects of combustor fluid dynamics with lean burn combustion systems considered as the principal solution for this problem. Computational fluid dynamics (CFD) simulations are often used in the gas turbine industry to predict and visualize the reacting flow dynamics and emission performance of combustors at the design stage and to assess new concepts. The combustor's reacting flow-field is in general turbulent and embraces many complex fluid dynamic phenomena. Hence, the CFD simulation of a gas turbine combustor is computationally very expensive. Due to the expensive nature of simulations, conventional techniques for CFD based combustor design optimisation are often ruled out, primarily due to the limits on available computing resources and time. Surrogate-based design optimisation techniques (including Kriging meta-models) have been used previously to accelerate the design optimisation process by reducing the total number of expensive CFD analyses. In this study, we develop and assess the performance of a multi-fidelity design strategy using co-Kriging surrogate modelling technique suitable for the design of a lean burn combustor using two levels of model analysis. Strategies with various combinations of low and high fidelity models are assessed.

Combustor model and reactive flow-field

A numerical study of turbulent reactive processes and NOx production behind a profiled backward-facing step in a two-dimensional test combustion chamber is presented. The test combustor modelled for the study is the one used by Keller et al., 1982 and Ganji et al., 1980 in an experimental study of mechanisms of instabilities in turbulent combustion leading to flashback.

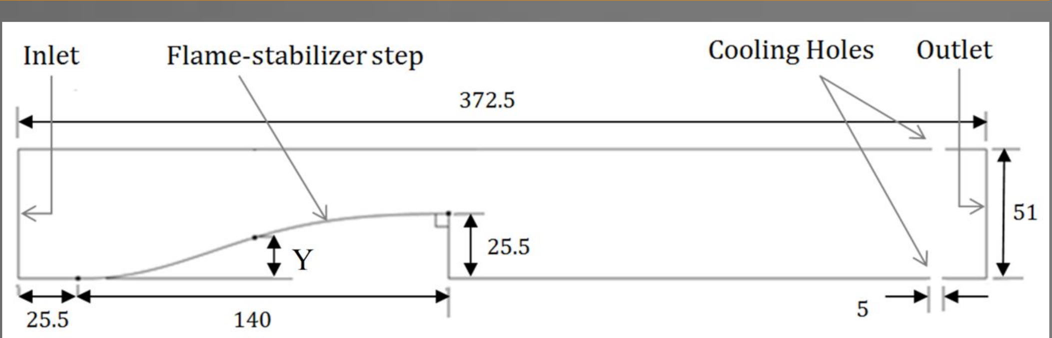

Figure 1. Computational domain of the combustor (All dimensions in mm)

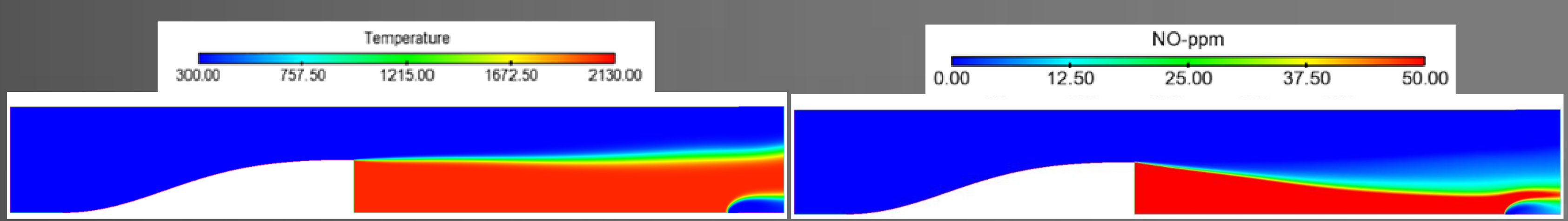

Figure 2. Temperature flow-field (left) and NOx production (right) behind the flame stabilizer step (steady RANS)

Figure 2 (left) shows the position of the flame surface inside the chamber obtained using steady RANS. As the Reynolds number of the flow is in the turbulent regime, the mixture burns only in the location where the turbulent flame speed S_T is able to sustain the inlet mixture velocity , i.e. the region behind the step. Therefore the chamber behind the step is separated into unburnt and burnt mixture regions by an interface, where combustion has started but not yet fully established. Above this surface, (C=0), the fuel and oxidizer mixture is mixed but unburnt, and below this surface (C= 1), the mixture is completely burnt. Figure 2 (right) shows the corresponding thermal NOx production behind the step. Thermal NOx formation rate is primarily a function of temperature and is produced only in the regions where the temperature is in excess of 1800 K

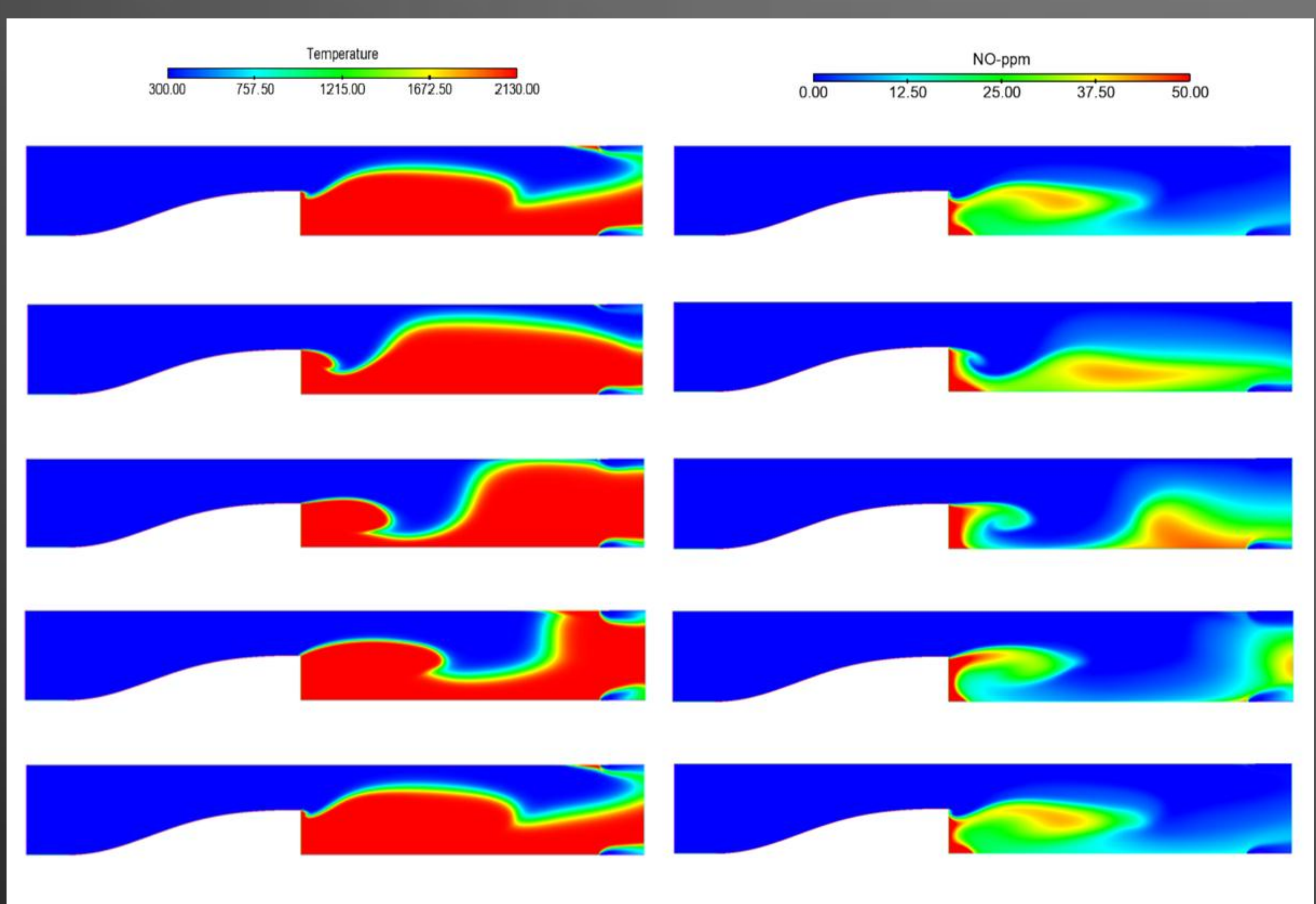

Figure 3. Humming instability cycle (left) and corresponding NOx variation (right) during the cycle (URANS @ Δt = 1e-05s)

Figure 3 (left) shows the images of the high frequency humming cycle captured using URANS. Burnt and unburnt mixture regions in the flow-field downstream of the step are clearly seen in Figure 3. The pulsation creates organized structures behind the step. This process is sustained in a meta-stable mode over a long period of time. Figure 3 (right) shows the formation of thermal NOx behind the flame stablizer step during the humming cycle. Thermal NOx concentration is observed to be higher in high temperature regions during the humming cycle and also appears to be en-trained by the vortices shedding behind the step.

Kriging and Co-Kriging based design optimisation strategies

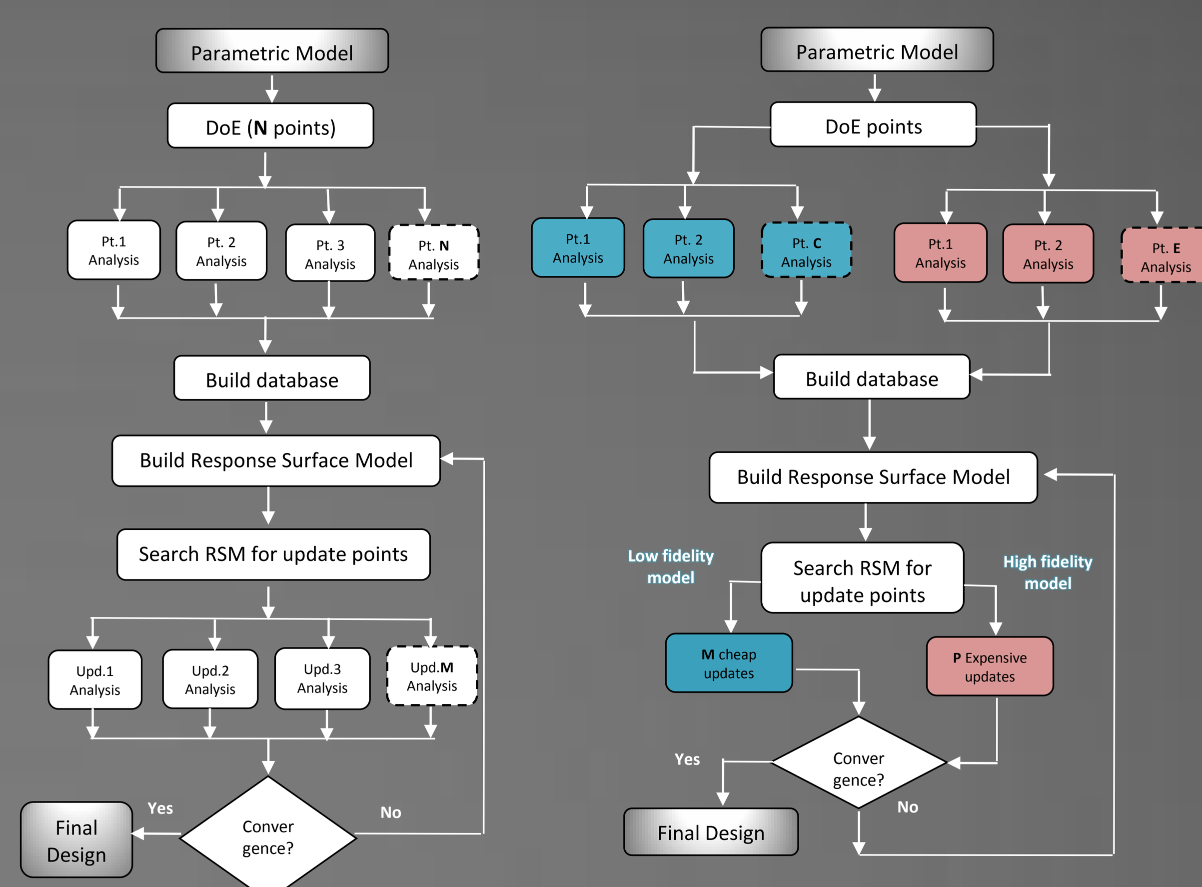

Figure 4. Kriging (left) and Co-Kriging (right) design strategies

Figure 4 (left) shows a traditional Kriging response surface model based design strategy with N Design of Experiments (DoE) points and M update points per update cycle. Figure 4 (right) shows a shows a co-Kriging response surface model based design strategy with **C** (cheap) and **E** (expensive) DoE points and **M** (cheap) and **P** (expensive) update points per update cycle, where **C** > **E** and M > **P**. An Expected improvement and best predicted point strategies are used to generate the update points in the design iterations. Both strategies are applied to optimize the flame stabilizer step design of the test combustor (c.f. Fig. 1) for minimum time-averaged NOx emission at the outlet using URANS analysis.

Figure 5 shows the NOx variation with the design space of two variables (Y and Theta) using a Kriging RSM of 100 CFD runs (10x10 regular grid data points). It shows a valley of low NOx value design configurations which becomes the area of attention when applying the strategies outlined in Figure 4. Starting from a 4 point optimal Latin Hypercube DoE, with a fixed computational budget of only 10 high fidelity CFD runs (URANS @ 1e-05s) or equivalent low-fidelity runs, both design strategies (c.f. Figure 4) are applied to find the best design configuration. Figure 6 shows the optimisation histories of Kriging strategy and various multi-fidelity co-Kriging strategies, within fixed computational budget, on nine different DoE samples.

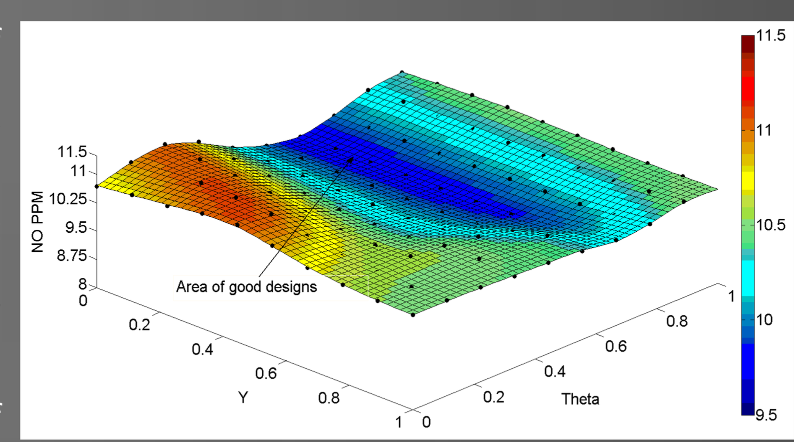

Figure 5. NOx variation within design space

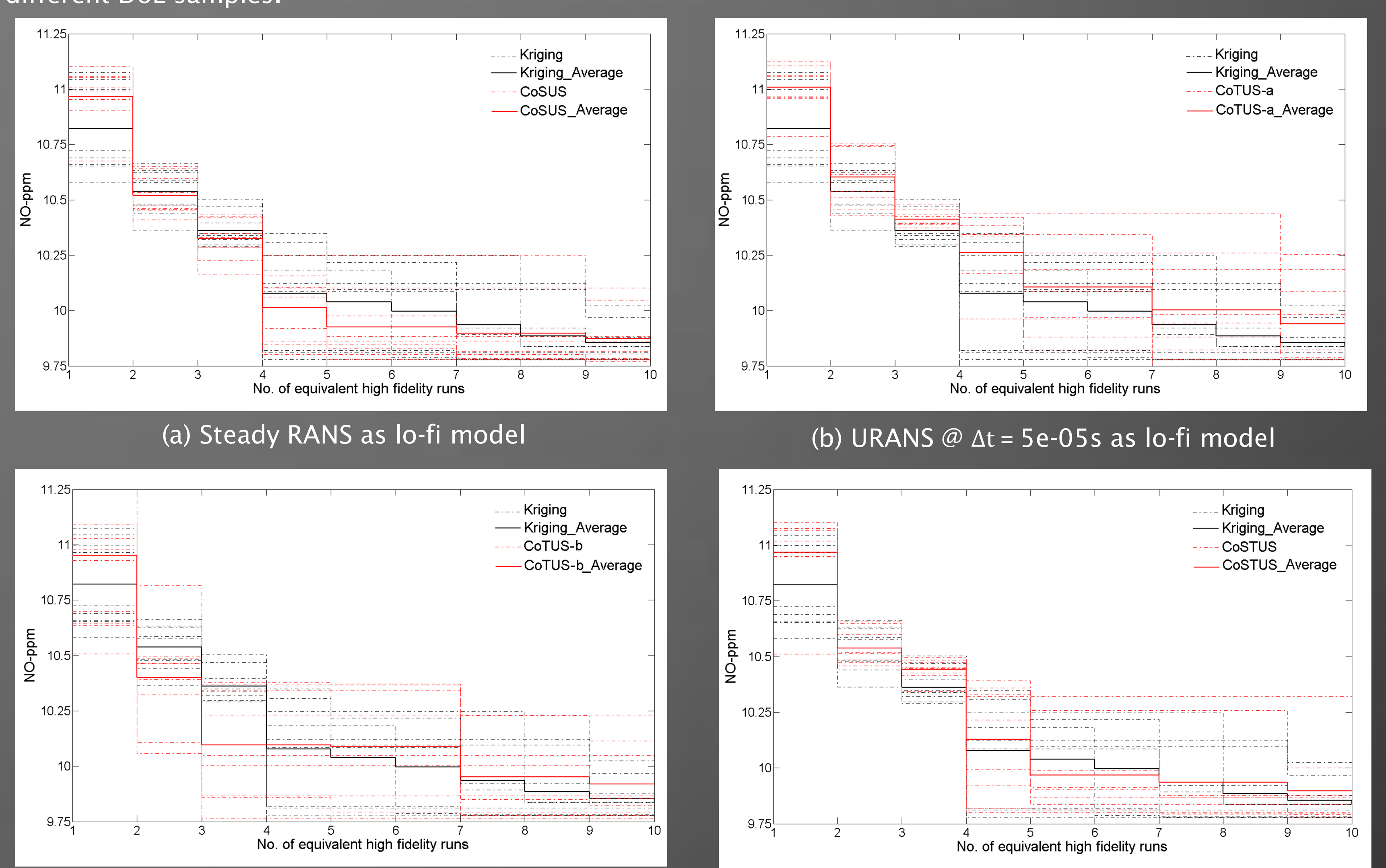

(a) Steady RANS as lo-fi model

(b) URANS @ Δt = 5e-05s as lo-fi model

(c) URANS @ Δt = 2e-05s as lo-fi model

(d) URANS @ Δt = 1e-04s on coarse mesh as lo-fi model

Figure 6. Optimisation histories of Kriging strategy and various co-Kriging strategies employing different low-fidelity (lo-fi) models in combination with fixed high fidelity model of URANS @ Δt = 1e-05s

Each design optimisation process is carried out on nine different DoE samples, with all nine optimisation histories plotted along with the respective mean. Different initial DoE's lead to different histories as information available at different locations in the design space causes different RSM convergence behaviour. However, from Figure 6, it is observed from the mean performances of both strategies in (a), (b), (c) and (d), that the multi-fidelity co-Kriging design strategy is competitive against the high-fidelity Kriging design strategy, with Kriging strategy generally performing better overall by the end of the fixed computational budget. However, it is also evident from the mean performance of strategy CoSUS (Figure 6(a)) and strategy CoSTUS (Figure 6(d)), that a good design is found early on in the design process, after the initial information obtained from the DoE runs.

Abbreviations:

RANS : Reynolds-Averaged Navier Stokes
URANS : Unsteady Reynolds-Averages Navier Stokes
RSM : Response Surface Model
CoSUS : **Co**-Kriging using **S**teady and **U**nsteady RANS **S**imulations on the same spatial grid
CoTUS : **Co**-Kriging using different **T**ime-steps of **U**nsteady RANS **S**imulations on the same spatial grid
CoSTUS : **Co**-Kriging using **S**patio-**T**emporal **U**nsteady RANS **S**imulations (coarse and fine, spatial and temporal grids)

www.soton.ac.uk/engineering/research/groups/CED/posters.page | email: nwb@soton.ac.uk
Computational Engineering & Design Group, University of Southampton, SO17 1BJ, U.K.